SEPARATE-EFFECTS EXPERIMENTS ON THE HYDRODYNAMICS OF AIR INGRESS PHENOMENA FOR THE VERY HIGH TEMPERATURE REACTOR

S. Kim[1], J. Talley[1], M. Yadav[1], A. Ireland[2], and S. Bajorek[2]
[1] The Pennsylvania State University, University Park, PA, USA
[2] The United States Nuclear Regulatory Commission, Washington, DC, USA
skim@psu.edu

Abstract

The present study performs scaled separate-effects experiments to investigate the hydrodynamics in the air-ingress phenomena following a Depressurized Condition Cooldown in the Very High Temperature Gas-Cooled Reactor. First, a scoping experiment using water and brine is performed. The volumetric exchange rate is measured using a hydrometer, and flow visualizations are performed. Next, Helium-air experiments are performed to obtain three-dimensional oxygen concentration transient data using an oxygen analyzer. It is found that there exists a critical density difference ratio, before which the ingress rate increases linearly with time and after which the ingress rate slows down significantly. In both the water-brine and Helium-air experiments, this critical ratio is found to be approximately 0.7.

Introduction

The DCC event is one of the most important design-based accident scenarios in a VHTR, which occurs under a postulated a double-ended guillotine break in the horizontal pipe connected to the lower section of the reactor vessel. When such an event occurs, the characteristic gravity-driven ingress of air (or Helium-air mixture) into the Helium filled reactor vessel occurs. This may result in the oxidation of graphite components producing CO and CO_2 gases, possible disintegration of the support structures and a release of fission gases.

The air-ingress phenomena can be characterized into three major stages based on the physical mechanisms: (1) During the first stage of air-ingress, cold air (or Helium-air mixture) inside the containment intrudes into the Helium-filled reactor vessel, driven primarily by the density difference. In this stage, the air fills the lower plenum of the vessel as the hot Helium gas escapes through the break. (2) Second stage of the ingress can be characterized by the thermally-driven exchange of gases. After the Helium-air mixture fills the bottom of the reactor vessel, temperature differences between the in-vessel Helium and the ex-vessel Helium-air mixture may induce exchange of gases due to the thermally-driven buoyancy force [1]. (3) As the ingress progresses further, the temperature difference in the gas mixture in the vessel may become large enough to trigger the natural circulation inside the reactor vessel. Hence, the final stage can be characterized by the massive air-ingress due to the natural convection inside the vessel [1-3].

The dominant mechanism during the immediate air-ingress following the depressurization has been widely debated in the past. Early studies focused more on molecular diffusion, ignoring the effects of buoyancy driven exchange flow [4-7]. However, the recent computational studies conducted by Oh et al. [1,8] suggests that the time scale for density driven exchange is approximately 800 times faster compared to the molecular diffusion. As such, the present study focuses to gain understanding on the gravity-driven exchange flows. More specifically, the primary goal of the current research is to perform separate-effects experiments on the hydrodynamic effects in the process of gravity-driven fluid ingress. This includes geometric effects, such as development length to break diameter ratio (L/D) and break orientations, pertinent to the VHTR air ingress condition.

Many experimental studies have been performed to investigate the density driven flow of a heavier fluid into a lighter fluid in the horizontal plane, referred to as the lock-exchange flow. Benjamin [9] developed a theory for the speed of the front depending on the depth of the current. Keller and Chyou [10] performed studies using several fluid pairs to formulate the hydraulic theory for lock-exchange flow covering the complete range of density ratios of $0<(\gamma = \rho_L/\rho_H)<1$. Two models were developed to account for different behaviors based upon the density ratio. For smaller density differences ($\gamma \geq 0.281$), the gravity currents connected by a long expansion wave with an internal hydraulic jump. However, for larger density differences ($0 < \gamma \leq 0.281$) the two fluids were connected only by a long expansion wave. Additional studies on the shape of the front and interface for lock-exchange with different density ratios were performed by Lowe et al. [11]. It was observed that for smaller density differences, the speed of both the currents were constant, nearly equal and that each fluid occupied approximately half of the channel. However, for the larger density differences, it was observed that while the speed of each current was constant, the heavier current traveled at a higher speed than the lighter current.

In order to investigate the effects of geometric parameters on the general flow characteristics resulting from buoyancy driven exchange, several previous studies have been performed using water and brine as simulant fluids. Leach and Thompson [12] investigated the effect of L/D in the range of 0.5 to 20. The exchange rate was expressed in terms of the Froude number, which scales the effect of inertia to buoyancy force. It was found that for horizontal flow, the exchange rate was not significantly affected by the L/D ratio, and that the Froude number was constant. A similar study on the L/D effect in vertical tubes was performed by Epstein [13] for L/D = 0.01 to 10 using water-brine. It was found that the Froude number increased with increasing L/D until reaching a maximum value at L/D = 0.6 and thereafter it decreased with further increase in L/D.

To investigate the effect of inclination angle, Mercer and Thompson [14] performed experiments using ducts inclined at various angles between the horizontal and vertical for varied L/D = 3.5 to 18. For a fixed L/D, the flow rate was found to increase as the duct angle increased from the horizontal up to a maximum value and then decreased to a minimum value for the vertical duct. Using Helium and air, Hishida et al. [15] covered a wide range of inclination angles from horizontal to vertical for L/D = 0.05 and 10 using rectangular geometry. The effect of L/D on Froude number was found to agree well with previous water-brine data. However, the angle of maximum exchange flow was found to be a strong function of L/D.

1. EXPERIMENTAL STUDY

Before performing the separate-effects tests using Helium and air, a scoping experiment is first performed by employing water and brine as a simulant fluid pair. The purpose of the scoping experiment is to gain physical understanding on the ingress processes via flow visualization and to characterize pertinent ingress phenomena through density measurements. In designing both test apparatuses, scaling studies are performed to preserve the major hydrodynamic effects that govern the exchange phenomena. As such, the water-brine experiment is developed to highlight flow visualization studies, while the Helium-air experiment presented in this paper is designed to focus on the hydrodynamics in the rupture of the horizontal primary inlet/exit duct or vertical standpipe, without including thermal driving effects.

1.1 Scaling Approach

In the current paper, only the adiabatic condition is presented to highlight the comparison between the Helium-air and water-brine systems with highly different density ratios (γ =0.14 and γ = 0.97, respectively). The test facilities are scaled using the GT-MHR conceptual design [16, 17] as a reference. This design has two major pipeline connections to the reactor vessel; the horizontal coaxial primary inlet/exit duct, and the vertical refueling standpipe. For initiation of an event leading to the ingress of air into the reactor vessel, these entry points of different size and orientation are considered. For the GT-MHR the diameter of the primary inlet pipe is given as 1.5 m, while the refueling standpipe is approximately 0.75 m in diameter.

In the scaling of gravity-driven exchange phenomenon, the previous studies suggest that the Froude number accounts for the effect of both break length and orientation [13-15]. The Froude number scales the inertia of the ingressing fluid with respect to the buoyancy induced by the fluid density difference and is given by:

$$Fr = \frac{Q}{A\sqrt{Dg\Delta\rho/\bar{\rho}}} = \frac{j}{\sqrt{Dg\Delta\rho/\bar{\rho}}} \tag{1}$$

where Q, A, D, $\Delta\rho$ and $\bar{\rho}$ denotes the volumetric exchange rate, break cross-section area, break diameter, density difference between the heavy and light fluids, and arithmetic mean of the fluid densities, respectively. The superficial fluid exchange velocity, j, is defined in the break by:

$$j_k = Q_k/A = \alpha_k u_k \tag{2}$$

where u denotes the fluid exchange velocity and α is the fraction of the cross-sectional area occupied by the fluid k. From the Equation (1), key scaling parameters are identified as:

$$Fr]_R = {Fr_{scaled}}/{Fr_{VHTR}} \quad \text{: Froude Number Ratio} \tag{3}$$

$$Q]_R = {Q_{scaled}}/{Q_{VHTR}} = \frac{Fr_{scaled}\left(\sqrt{D^5 g\Delta\rho/\bar{\rho}}\right)_{WB}}{Fr_{VHTR}\left(\sqrt{D^5 g\Delta\rho/\bar{\rho}}\right)_{HA}} \quad \text{: Global Exchange Ratio} \tag{4}$$

$$j]_R = {j_{scaled}}/{j_{VHTR}} = \frac{Fr_{scaled}\left(\sqrt{Dg\Delta\rho/\bar{\rho}}\right)_{WB}}{Fr_{VHTR}\left(\sqrt{Dg\Delta\rho/\bar{\rho}}\right)_{HA}} \quad \text{: Local Exchange Ratio} \tag{5}$$

$$t]_R = {t_{scaled}}/{t_{VHTR}} = \frac{\left({V}/{Q}\right)_{scaled}}{\left({V}/{Q}\right)_{VHTR}} \quad \text{: Exchange Time Ratio} \tag{6}$$

where the subscripts *scaled* and *VHTR* denote the scaled experiment and the VHTR geometry under the adiabatic condition, respectively. Based on the two entry locations in the GT-MHR vessel, different amounts of fluid volume, V, can be exchanged depending upon the vessel volume below the break location. In the vertical standpipe case, a complete vessel volume exchange is assumed, such that the heavier air in containment will completely displace the lighter Helium in the reactor vessel. For the primary break case, the air is assumed to displace any Helium below the plane parallel to the top of the primary pipe break. The volume occupied by the core region is considered, however in the experimental facilities the scaled volume is treated as unoccupied space to simplify design. Future experiments are planned to account for the internal geometry of the VHTR.

In view of the viscous forces, the Reynolds number is also considered in the scaling analysis. It should be noted, however, that both Epstein [13] and Hishida et al. [15] observed that the flow structure and exchange mechanisms depended primarily on the L/D ratio in a vertical break. Hence, only the lock-exchange flow is considered in examining the Reynolds number. Here, the Reynolds number is defined through the superficial velocity, j, as $Re = \rho jD/\mu$, where D is the break diameter. Using Equation (1) and the previous studies [13-15], j is estimated through the Froude number. In the scaling analysis, Equation (6) is selected as the primary ratio as it scales the total estimated time for the ingress to occur. This information is important in view of mitigation procedures to reduce possible damage to the graphite materials from oxidation. In view of focusing on the Helium-air experiment, only the scaling ratios for that facility are discussed in Section 2.3. A detailed discussion on the water-brine scaling results can be found in the work of Sarangi [18].

1.2 Water-Brine Scoping Study

The scoping apparatus consists of two narrow rectangular acrylic tanks of dimensions 25.4 x 25.4 x 3.81 cm. The narrow rectangular geometry is chosen to highlight two-dimensional mixing and enhance flow visualization studies. The width of the compartment is chosen to be at least 10 times the break diameter (1.9 cm) to minimize any wall effects in the direction of the width. These compartments are connected by pipes of length 0.63, 3 or 5 diameters. For the GT-MHR, the length of the primary pipe between the reactor vessel and the power conversion unit is approximately 4.5 meters, or 3 diameters. To investigate the effect of break angle, the test apparatus is attached to a pivoting support structure, which can be locked at any position between vertical and horizontal within ±0.1°. The initial density difference between the fluids is chosen to be in the range of $\Delta\rho/\bar{\rho}$ =0.025-0.030 to be consistent with the studies by Epstein [13] and Mercer and Thompson [14]. To initiate the ingress at the beginning of a test, a sliding gate mechanism is employed to minimize the disturbance to the flow.

The flow visualization study is performed by dying the brine a darker color to distinguish the interface between the fluids. It is observed that the mixing phenomenon is highly dependent on the angle of inclination. For the horizontal break when the gate is opened, the fluid propagates from the brine compartment to the water compartment with a well-defined front or nose. Following the nose, a stable interface between the brine and water is observed. The propagation fronts of brine and water are symmetric about the center of the pipe break axis and occupy approximately half of the depth of the pipe.

Upon entering the lower compartment the brine forms a traveling layer along the bottom as shown in Figure 1 (a). This layer is observed to have a greater thickness at the front as compared to the trailing edge and can be considered a hydraulic jump. Once the brine reaches the wall, it is forced upward by the ingressing brine, as shown in Figure 1 (b). The brine that is forced upward cannot fall back down due to the continuously ingressing brine. Instead the wave propagates back across the compartment towards the break. This characteristic wavy mixing phenomenon, as shown in Figure 1 (c), occurs until the heavier fluid reaches the break height.

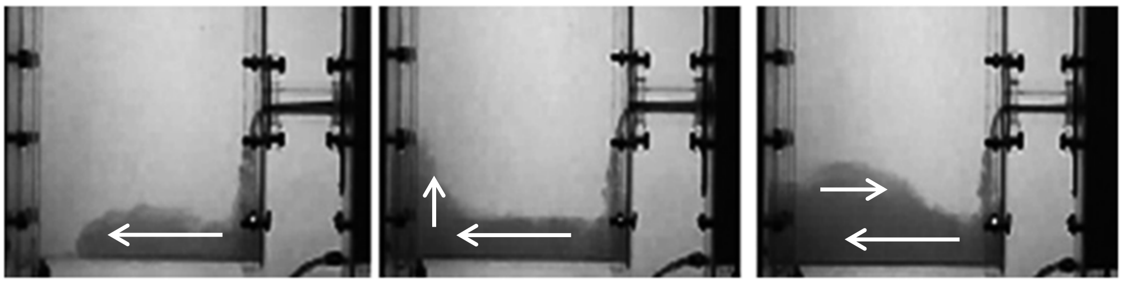

(a) **(b)** **(c)**

Figure 1 Water-brine visualization study, time progression in horizontal ingress of more dense brine (dark fluid) into less dense water.

For the vertical pipe break, as shown in Figure 2 (a), that there is no clear stable interface between the fluids and the mixing phenomena is highly three-dimensional. The fluid streams interact strongly and fluctuate irregularly. Moreover, this three-dimensional mixing causes a significant reduction in the ingress rate as compared to the horizontal case. Flow visualization shows that as the brine ingresses into the lower compartment, the plume spreads and the outer region is slowed by the shear flow with the stagnant water. This slower region is then displaced outward by the continuously ingressing plume as seen in Figure 2 (b), and the brine spreads throughout the compartment rapidly on the order of 1 to 2 minutes. In all the cases, it is observed that the ingress rate decreases after the brine has spread throughout the compartment.

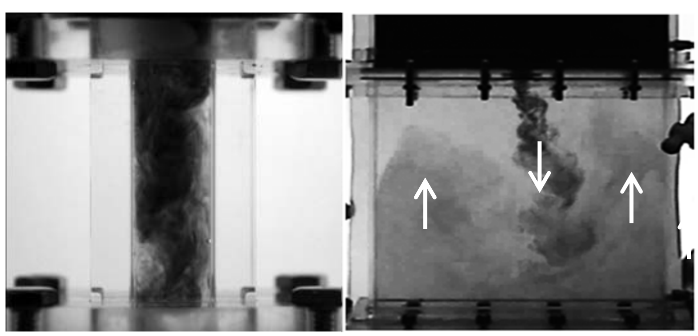

(a) **(b)**

Figure 2 Water-brine visualization study: vertical ingress of more dense brine (dark fluid) into less dense water. Flow structure in (a) break pipe and (b) mixing compartment.

An example of a density measurement obtained using a hydrometer in the compartment initially filled with brine is shown in Figure 3 for the horizontal ingress with L/D=3. From the Figure it is observed that the data can be divided into two regions. In the initial region, the change of density is linear with respect to time, while in the subsequent region the density change becomes non-linear. This phenomenon is observed for all flow conditions.

The flow visualization shows that this transition corresponds to the time when the brine in the water compartment reaches the break height. After this transition occurs, the ingress rate slows as the density difference between the fluid compartments decreases. In this second region, the data is well correlated by a logarithmic decay relation as shown in Figure 3(b). Furthermore, the transition point is found to be related to the density difference ratio given by:

$$\rho^*_{tr,i} = \frac{\Delta\rho_{tr,i}}{\Delta\rho_i} = \frac{(\rho_H)_{tr,i} - (\rho_L)_{tr,i}}{\rho_{H,i} - \rho_{L,i}} = 0.74 \pm 5\% \tag{7}$$

where ρ_L is the density of the lower compartment and $\rho^*_{tr,i}$ is the density difference at the point of transition normalized with respect to the initial density difference. The value of this parameter is found to be within the same range for all 21 break angle and length combinations investigated.

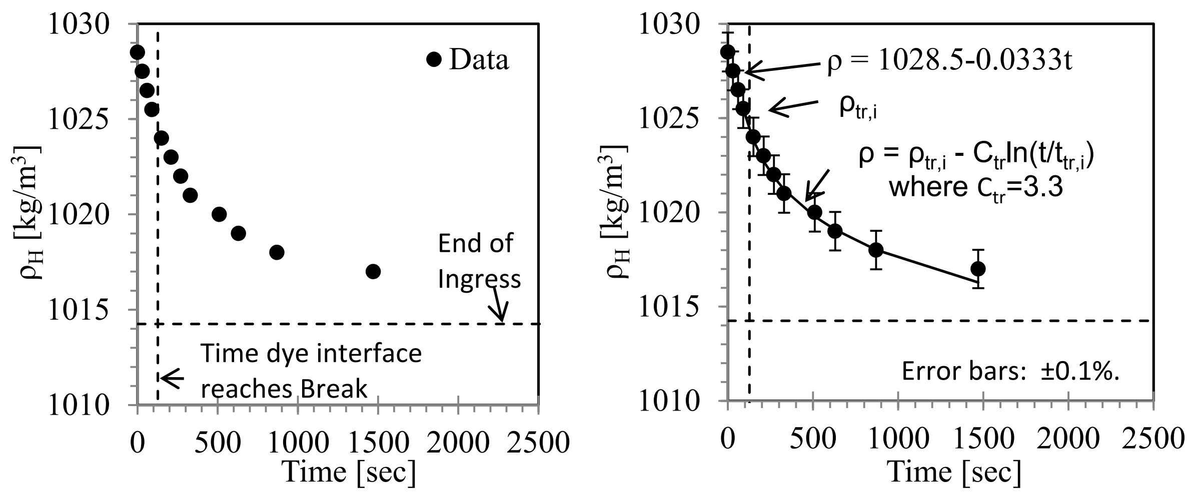

(a) Measured density transient. **(b) Two region correlation.**

Figure 3 Density change in brine compartment during horizontal ingress for L/D=3.

1.3 Adiabatic Helium-Air Study

Based on the observations of the scoping experiment, a Helium-air experimental facility is established to develop a database for gravity driven exchange flow in a higher density difference flow condition. The experimental vessel is constructed with diameter of 61 cm and height of 183 cm as shown in Figure 4. The vessel has three break locations: one centered on the top plate and two on the side of the vessel centered at 11.4 cm and 34.3 cm from the bottom of the vessel, respectively. The top plate location is designed to simulate a break in the refueling standpipe, while the lower horizontal break is designed to simulate a break in the primary coolant pipe of the GT-MHR. Flanged pipes can be attached at any break location to investigate the geometric effects of different L/D ratios and inclination angle. Only adiabatic testing ($\gamma = 0.14$) simulating the primary pipe break is discussed in this work.

With the given vessel geometry, the scaling ratios are shown in Table 1. As in the water-brine experiment, Equation (6) is selected as the primary ratio to match to be of order unity. In the analysis it is assumed that the unheated and heated conditions have the same Froude number as no heated experimental data is available. In Table 1 the Reynolds number ratio deviates from unity and it is recognized that the viscous effects in the experiment can be greater than that in the prototypic condition. However, as the previous studies suggest that the Froude number captures the effect of the density driven flow, it is chosen as the primary non-dimensional number to preserve. Hence, it is necessary to distort the Reynolds number ratio to preserve the Froude number ratio as unity. Details of the scaling analysis can be found in the work by Baird [19].

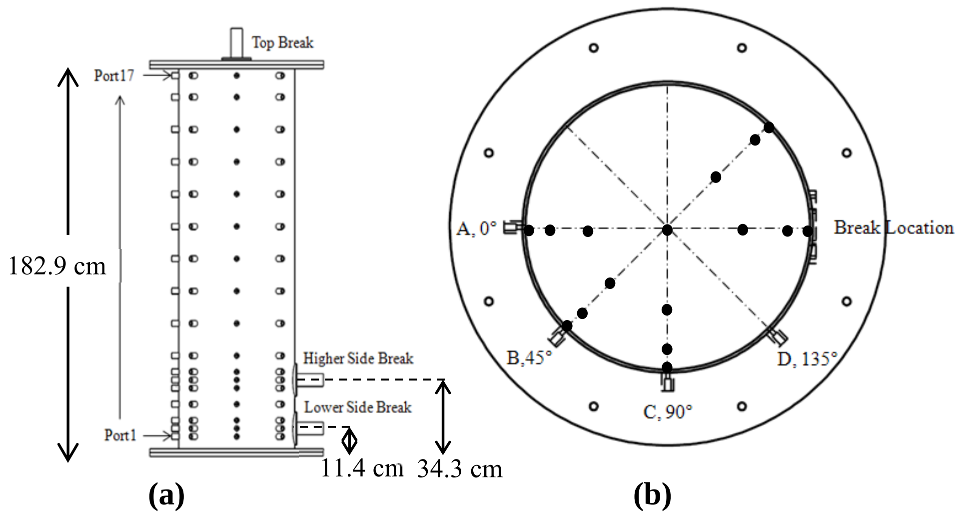

Figure 4 Schematic diagram of Helium-air test facility.
(a) Side view and (b) top view with radial measurement locations.

Table 1 Helium-Air scaling ratios for horizontal and vertical breaks.

	$Fr]_R$	$Q]_R$	$j]_R$	$t_G]_R$	$Re]_R$	Diameter, cm
Horizontal Break	1.00	1.90E-4	0.166	2.29	6.24E-3	5.08
Vertical Break	1.00	1.08E-3	0.235	1.41	--	5.08

A total of 68 instrumentation ports are available on the vessel to sample the local gas mixture using an Ametek Thermox CEM O_2/TM Trace Oxygen Analyzer. The analyzer pulls a continuous sample and has a measurement range from 1 ppm O_2 to 100% O_2 with a maximum accuracy level of ±0.75% O_2. The instrumentation ports are located radially at four azimuthal locations of 45°, 90°, 135°, and 180° from the horizontal break axis to allow measurement over the entire vessel cross-section. A total of 17 axial levels are employed to capture the axial evolution of the ingress.

Prior to an experiment, the sampling probe is positioned at a measurement location of interest, a break pipe is installed and a silicone plug is installed to seal the break. Air in the vessel is evacuated using a vacuum pump and then filled with Helium to a pressure of approximately 7,000 Pa. This pressure is chosen, such that when the plug is removed to initiate the ingress event, the tail end of the depressurization stage is simulated. During the experiment the transient trace of the local oxygen concentration is recorded. Therefore, 3-D transient oxygen concentration profiles can be generated through repetition of the same break condition at different local sampling positions.

For L/D=3, the horizontal ingress experiment is repeated at 16 radial positions for three axial locations to map the air concentration during the ingress event. The concentration profiles obtained at Port 1 (1.3 cm below the lower side break) are shown in Figure 5. Very near the break location, a greater air concentration is observed, and can be observed far into the ingress event. In general, however, for a given axial elevation the measured radial concentrations are nearly identical indicating the air is well mixed with the helium as it settles in the vessel.

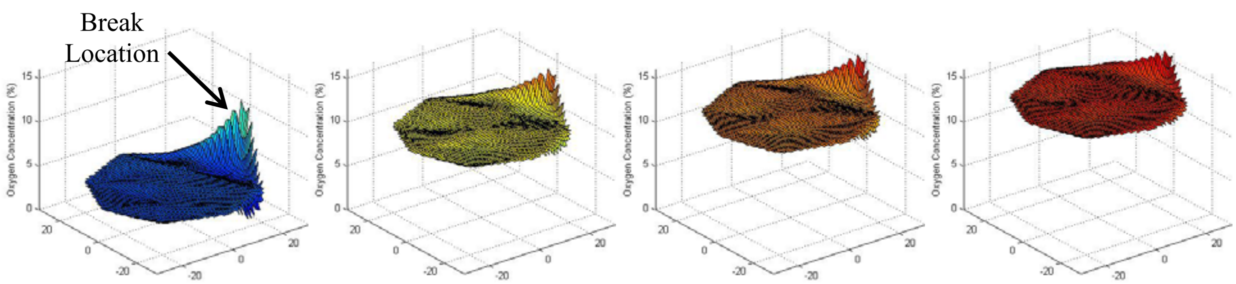

100 seconds **300 seconds** **500 seconds** **1000 seconds**

Figure 5 Progression of measured air concentration at axial plane Port 1 (1.3 cm below break) for L/D=3 horizontal Helium-air test.

An example of local radial measurements at a fixed axial elevation is shown in Figure 6 for three radial locations: 1.3, 5.1 and 17.8 cm from the break, respectively. As the oxygen concentration in air is approximately 21%, the oxygen profiles can be employed to obtain the air concentration behavior. From the Figure it can be observed that the two positions 5.1 cm and 17.8 cm behave almost identically as in the previous Figure. Near the break, however, a different phenomenon is observed. It is found that the air concentration increases at this location earlier and faster compared to the other sampled locations. Moreover, this curve displays oscillations in the air content. To verify this oscillatory behavior, the nearest radial location is sampled multiple times with the same behavior observed in each run. Hence, it is speculated that at the radial location of 1.3 cm from the break, the probe is sampling near the air plume boundary. As observed in Figure 1 with the water-brine study, the interface between the fluids can contain disturbances as they flow past one another.

The plane averaged concentrations can be obtained as shown in Figure 7. Air is first detected at the lowest axial position and then progressively detected at the higher elevations as time increases. Therefore, it can be observed that a nearly uniform Helium-air mixture progresses upward as time progresses. At each axial elevation, the initial linear region followed by a non-linear region is also observed. It can also be noted that as time increases the averaged values at each elevation are converging, indicating the trend toward a fully mixed condition in the vessel.

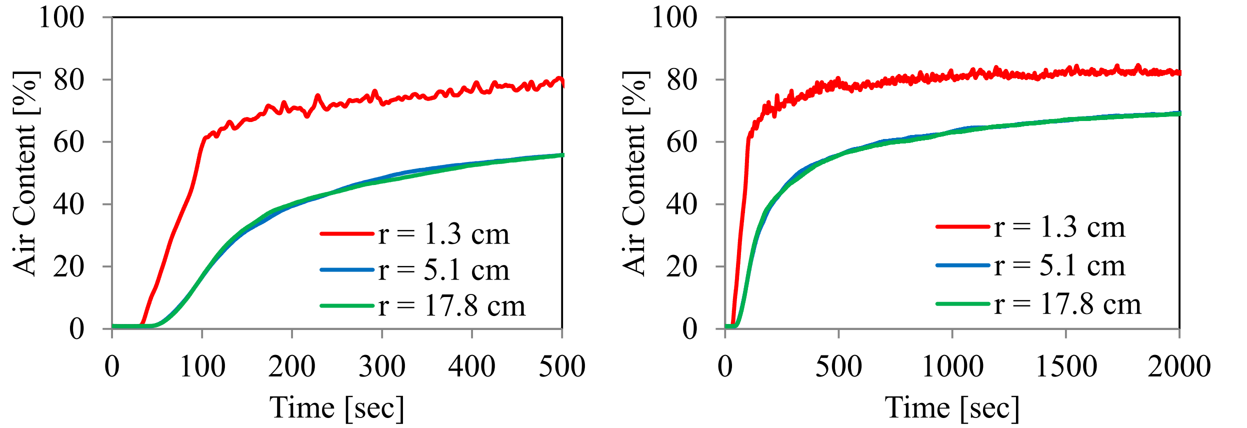

Figure 6 Local measurements of radial air concentration at Port 1 (1.3 cm below break) for L/D=3 horizontal Helium-air test. Position denotes radial distance from the break.

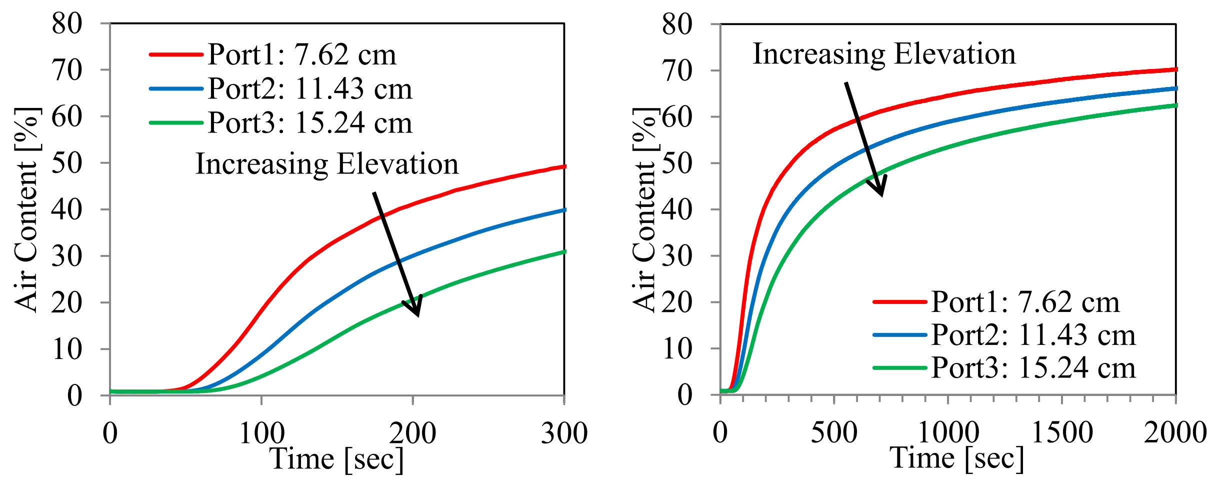

Figure 7 Measured area-averaged air concentration for L/D=3 horizontal Helium-air test at three axial elevations.

While Figures 3 and 7 show similarity in the ingress nature, a more direct comparison between the density transients of the two systems is shown in Figure 8. Both the Helium-air and water-brine density values are normalized using Equation (7) for time t instead of the transition time, tr,i. Here, the water-brine lower compartment density is obtained using conservation of mass. The time scale of the experiment is employed since in both systems this of the order of unity with the VHTR system. In Figure 8, it is clear that the ingress nature of the two systems is similar. For the linear region, where the ingress rate is largest, the exchange time ratio of Equation (6) is of the order of unity, the two systems are nearly identical. In addition, the transition points between the linear and non-linear regions for both systems are also found to be very similar. For all the water-brine scoping studies and the preliminary Helium-air tests, the average transition value is found to occur at $\rho^*_{tr,i}$ = 0.74 and 0.72, respectively. Therefore, regardless of the large density difference, this criterion appears to remain nearly constant. As the two experimental systems are found to deviate in the non-linear region, it is recognized that a similar deviation to the VHTR condition could occur. However, from Figures 6 and 7, high air concentrations are observed after the relatively short linear region. Hence, mitigation may be necessary before the systems deviate.

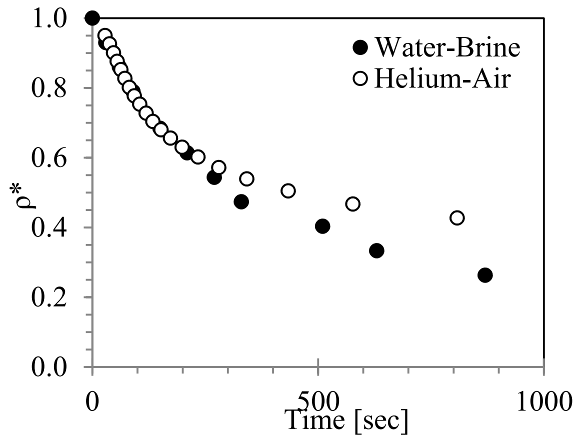

Figure 8 Comparison of experimental systems for L/D=3 horizontal condition.

The volumetric flow rate can be obtained by determining the change in the volume of air in the system. This calculated volumetric flow rate for the horizontal break with L/D=3 is shown in Figure 9. It is observed that the ingress rate initially increases rapidly, followed by a sharp decrease which then asymptotes to a zero ingress rate at the completion of the event. It can be observed that the time at which this inflection occurs corresponds to the time when the change in the air concentration becomes non-linear. This result differs from the previous studies [13-15], where the volumetric flow rates were reported to be a constant value. However, if the current data is time-averaged, it is found to agree well with that of Hishida [15] as shown in the Figure. Hence, it is observed that current result highlights the mixing volume effect whereas the previous studies did not.

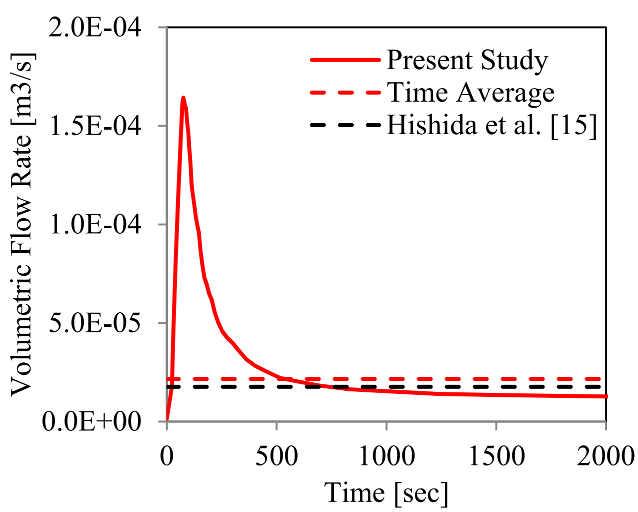

Figure 9 Calculated transient air ingress rate for horizontal primary break with L/D=3.

2. SUMMARY

The present study performs separate-effects experiments to investigate the hydrodynamics in the ingress process by employing two different pairs of simulant fluids under the room temperature condition, namely water-brine and Helium-air. Both systems are scaled using the GT-MHR design to maintain a time scale on the order of unity where both the horizontal primary break and vertical stand pipe ruptures are considered. First, a water-brine scoping experiment is performed to gain understanding of the ingress characteristics through both flow visualization and density measurements. In the flow visualization study it is observed that the mixing phenomenon is highly dependent on the angle of inclination as well as the compartment geometry. Initially, the ingress rate linearly increases followed by a logarithmically decaying region. From the flow visualization study, it is found that this transition occurs when the heavier ingressing fluid fills to the break location.

In the adiabatic Helium-air experiments, where the density difference is much greater, three-dimensional transient air concentration profiles are obtained through measurement via an oxygen analyser at multiple radial and axial positions. For the primary pipe break experiment, it is found that for a given axial elevation the radial concentrations are nearly identical except near the ingress location. Hence, it is observed that the ingressing air is well mixed with the Helium in the vessel below the break. It is also found that the Helium-air data shows the same characteristic linear and non-linear regions as the water-brine scoping experiment. Moreover, despite the large difference in density ratios between the water-brine and Helium-air systems, both exhibit nearly the same transition point to the non-linear region at a value of approximately $\rho^* = 0.7$. This transition is contrary to the previous studies, where the ingress rate was reported as constant. It is speculated that in previous studies the use of larger mixing volumes did not capture the non-linear region of the ingress. Therefore, the current study captures the effect of density-driven mixing in finite volumes more applicable to the VHTR condition.

3. References

[1] Oh. C., and Kim, E., “Air-ingress analysis: Part 1 – Theoretical Approach,” *Nuc. Eng. Des.*, 241, 2011, 203-212.

[2] Hishida, M., and Takea, T., “Study on air ingress during an early stage of a primary-pipe rupture accident of a high-temperature gas-cooled reactor,” *Nuc. Eng. Des.*, 126, 1991, 175-187.

[3] Takeda, T., and Hishida, M., “Studies on diffusion and natural convection of two component gases,” *Nuc. Eng. Des.*, 135, 1992, 341-354.

[4] Takeda, T., “Air ingress behavior during a primary-pipe rupture accident of HTGR,” Japan Atomic Energy Research Institute, JAERI-1338, 1997.

[5] Takeda, T., and Hishida, M., “Studies on molecular diffusion and natural convection in a multicomponent gas system,” *Int. J. of Heat and Mass Transfer*, 39, 1996, 527-536.

[6] Oh., C. H., et al., “Development of safety analysis code and experimental validation for a Very High Temperature Gas-Cooled Reactor,” Idaho National Laboratory, INL/EXT-06-01362, 2006.

[7] No, H. C., Lim, H. S., Kim, J., Oh, C., Siefken, L., and Davis, C., "Multi-component diffusion analysis and assessment of GAMMA code and improved RELAP5 code," *Nuc. Eng. Des.*, 237, 2007, 997-1008.

[8] Oh., C. H., Kim, E. S., Kang, H. S., No, H. C., and Cho, N. Z., "Experimental validation of stratified flow phenomena graphite oxidation and mitigation strategies of air ingress accidents, FY-09," Idaho National Laboratory, INL/EXT-09-16465, 2009.

[9] Benjamin, T. B., "Gravity currents and related phenomena," *J. Fluid Mech.*, 31, 1968, 209-248.

[10] Keller, J. J., and Chyou, Y. –P., "On the hydraulic lock-exchange problem," *J. Appl. Math. Phys.*, 42, 1991, 874-910.

[11] Lowe, R. J., Rottman, J. W., and Linden, P. F., "The non-Boussinesq lock-exchange problem. Part 1. Theory and Experiments," *J. Fluid Mech.*, 537, 2005, 101-124.

[12] Leach, S. J., and Thompson, H., "An investigation of some aspects of flow into gas cooled nuclear reactors following an accidental depressurization," *J. Br. Nuc. Energy Soc.*, 14, 1975, 243-250.

[13] Epstein, M., "Buoyancy-driven exchange flow through small openings in horizontal partitions," *J. of Heat Trans.*, 110, 1988, 885-893.

[14] Mercer, A., and Thompson, H., "An experimental investigation of some further aspects of the buoyancy-driven exchange flow between carbon dioxide and air following a depressurization accident in a Magnox Reactor, Part I: The exchange flow in inclined ducts," *J. Br. Nuc. Energy Soc.*, 14, 1975, 327-334.

[15] Hishida, M., Fumizawa, M., Takeda, T., Ogawa, M., and Takenaka, S., "Researches on air ingress accidents of the HTTR," *Nuc. Eng. Des.*, 144, 1993, 317-325.

[16] MacDonald, P. E., et al., "NGNP point design – results of the initial neutronics and thermal hydraulic assessments during FY-03," Idaho National Laboratory, INEEL/EXT-03-00870, 2003.

[17] Richards, M. B., et al., "H2-MHR pre-conceptual design report: SI-based plant," General Atomics, GA-A25401, 2006.

[18] Sarangi, S., "Scaled Experiment on Gravity Driven Exchange Flow for the Very High Temperature Reactor," M.S. Thesis, The Pennsylvania State University, 2010.

[19] Baird, J. J., "Scaled Experiments on Air Ingress in the Very High Temperature Reactor (VHTR)," M.S. Thesis, The Pennsylvania State University, 2010.